ELSEVIER

Aquacultural Engineering 25 (2002) 217–237

aquacultural engineering

www.elsevier.com/locate/aqua-online

Prediction of aeration performance of paddle wheel aerators

Sanjib Moulick, B.C. Mal *, S. Bandyopadhyay

Aquacultural Engineering Section, Agricultural and Food Engineering Department, IIT, Kharagpur 721 302, West Bengal, India

Received 31 March 2001; accepted 3 September 2001

Abstract

Aeration experiments were conducted in brick masonry rectangular tanks of dimensions $2.9 \times 2.9 \times 1.6$ and $5.9 \times 2.9 \times 1.6$ m to study the effect of geometric and dynamic variables on aeration process based on dimension analysis. Non-dimensional numbers relating to standard aeration efficiency (SAE), effective power (P) and theoretical power per unit volume (P/V) termed as SAE′, *Ne* and *X*, respectively, are proposed. An optimal geometric similarity of various linear dimensions was established. It has been established that neither the Reynolds criterion nor the Froude criterion is singularly valid to simulate either SAE′ or *Ne*, simultaneously for different sizes of aerators, even though they are geometrically similar. Occurrence of scale effects due to the Reynolds and the Froude laws of similitude on both SAE′ and *Ne* are also evaluated. Simulation equations uniquely correlating SAE′, *Ne* and X were developed which can predict the aeration performance of paddle wheel aerators having the optimised geometric dimensions as established.

Keywords: Paddle wheel aerator; Similarity criteria; Dimensionless numbers; Aeration performance

1. Introduction

The intensive fish culture system often needs the introduction of artificial aeration systems (Boyd and Ahmad, 1987). These systems vary from emergency aeration, operated only when the oxygen level drops to dangerous values, through ordinary

* Corresponding author. Tel.: +91-3222-83128; fax: +91-3222-82244.
E-mail address: bmal@agfe.iitkgp.ernet.in (B.C. Mal).

0144-8609/02/$ - see front matter
PII: S0144-8609(01)00087-5

night-time aeration, to continually operating aeration systems in highly stocked ponds. The obvious role of aeration is to supply oxygen to fish. In addition, aeration of the water may affect a variety of other biological systems in the pond. In the biological treatment of wastewater, aeration is an important process employed to raise the dissolved oxygen (DO) level to allow aerobic bacteria to reduce biochemical oxygen demand of the effluent and thus to improve the water quality. The oxygen supplied must be at a rate sufficient to at least balance the rate of removal of the active biomass. Aerators are the devices used to supply oxygen to meet such demands.

An electric paddle wheel aerator consists of a motor, a speed reduction mechanism, and paddle wheel mounted on a floatation device. The oxygen transfer efficiency of a paddle wheel aerator depends upon design and operating characteristics of the paddle wheel. The paddle wheel is rotated to create turbulence in the water body so that aeration takes place through the interface of atmospheric air and water surface. The rate of oxygen transfer depends on the intensity of turbulence created in the water body. The intensity of turbulence, in turn, depends on the speed of rotation, size, shape and number of blades, diameter and immersion depth of the rotor, and size and shape of aeration tank, as well as on the physical, chemical, and biological contents/properties of water.

Aeration performance tests in tanks (Boyd and Ahmad, 1987) indicate that paddle wheel aerators are more efficient in transferring oxygen and circulating water than other types of aerators commonly used in aquaculture. Rappaport et al. (1976) made pond tests of several aeration systems (paddle wheels, aspirator, vertical pump and diffused-air), and found that paddle wheel aerators were much more efficient than the other types. For aerators of 1 kW and larger, paddle wheel aerators are equal or less in cost than other types of aerators. However, small paddle wheel aerators are more expensive than other types of small electric aerators, because gearmotors required for small paddle wheel aerators are very expensive.

If world-wide usage of aerators is considered, the small paddle wheel aerators which are manufactured in Taiwan, probably dominate the market. These aerators are not as efficient as some other types of paddle wheel aerators, but they are relatively inexpensive, lightweight, of suitable size for intensive ponds, corrosion resistant, and well known (Boyd, 1998). Taiwanese paddle wheel aerators are extremely popular for use in intensive shrimp culture ponds in Asia (Wyban et al., 1989). Ahmad and Boyd (1988) tested several designs of paddle wheel aerator and found that a 91 cm diameter paddle wheel with triangular paddles (120–135°) operated at 77 rpm and 12.5 cm paddle submergence depth offered the highest standard aeration efficiency (SAE) (2.96 kg O_2/kW h). Moore and Boyd (1992) provided equations to assist in the design of small (0.18–1.5 kW) paddle wheel aerators within the range studied. Furthermore, information on horizontal rotor aerators used in wastewater treatment (Walker, 1962; Knight, 1965; Cleasby and Baumann, 1968; Kolega et al., 1969) is not directly applicable to fish pond aerators.

In the field of wastewater treatment, many investigators have successfully made use of the theory of dimensional analysis and obtained optimal geometric similarity

of horizontal rotor aerators under different conditions (Zlokarnik, 1979; Eckenfelder, 1956; Horvath, 1984; Schmidtke and Horvath, 1976; Banks et al., 1983; Simha, 1991; Ognean, 1993). All the studies conducted in aquaculture field dealt only with the design and manufacturing aspect of the paddle wheel aerator and it is quite amazing to see that there are still no correlations for prediction of aeration performance of the paddle wheel aerators. From the review of the available literature it is observed that geometric and dynamic similarities have to be established to simulate the process of aeration in tanks of different sizes and shapes and under different dynamic conditions. For such a simulation, dimensional analysis of various geometric, dynamic, and physical variables plays a significant role (Rao, 1999).

The results of the study of a paddle wheel aerator having different shapes and sizes under geometrically similar conditions are presented in this paper. An optimal geometric similarity is established. Occurrence of scale effects due to the Reynolds and the Froude laws of similitude are presented and finally simulation equations to predict the aeration performance under geometric similar conditions are developed.

2. Theoretical consideration

According to two-film theory (Lewis and Whiteman, 1924; Eckenfelder and O'Conner, 1961; Cleasby and Baumann, 1968; Metcalf & Eddy Inc., 1979; Manual 1988), mass transfer occurs through the gas and liquid interface, through a laminar flow in the two films (one gas and one liquid) and through turbulent flow in the body of the liquid until a dynamic equilibrium is established. The rate of mass transfer, $\partial m/\partial t$ of oxygen from the atmosphere to the body of the turbulent liquid generally is proportional to the difference between the existing concentration C and the equilibrium or saturation concentration C^* of oxygen in the liquid. It can be expressed as $\partial m/\partial t = k_L A(C^* - C)$, where k_L = coefficient of diffusion of oxygen in the liquid; and A = area through which oxygen is diffusing. By noting $\partial m/\partial t = V(\partial C/\partial t)$, where V = volume of the liquid, then it can be expressed as $\partial C/\partial t = (k_L A/V)(C^* - C)$. The parameter $k_L A/V$ is generally designated by $k_L a_T$, the overall oxygen transfer coefficient at test temperature T (°C). Integrating the equation between the limits $C = C_0$ at time $t = 0$ and $C = C_t$ at $t = t$, one obtains

$$K_L a_T = [\ln (C^* - C_0) - \ln (C^* - C_t)]/t \quad (1)$$

where ln represents natural logarithm of the given variables and the concentrations C^*, C_0, and C_t are usually expressed in parts per million (ppm). The value of $k_L a_T$ can be obtained as equal to the slope of the linear plot between $\ln (C^* - C_t)$ and the corresponding time t. The value of $k_L a_T$ thus obtained is to be converted to a value at a standard temperature of 20 °C as $k_L a_{20}$, called the overall oxygen transfer coefficient under standard condition, for the purpose of comparison of results, by the following equation (Manual 1988):

$$(k_L a)_{20} = \frac{(k_L a)_T}{\theta^{T-20}} \quad (2)$$

where θ is 1.024 for pure water.

Thereby the standard oxygen transfer rate (SOTR) in kg O_2 h^{-1} can be estimated by the following equation

$$\text{SOTR} = (k_L a)_{20} \times 9.07 \times V \times 10^{-3} \quad (3)$$

where 9.07 = saturated DO at 20 °C and standard atmospheric pressure, V = aeration tank volume (m^3) and 10^{-3} = factor for converting gram to kilogram. It is an important parameter used to compare aerators. In most cases larger aerators will transfer more oxygen than smaller ones. A better comparative parameter is the SAE which is defined as the amount of oxygen transferred per unit of power. SAE is calculated by

$$\text{SAE} = \frac{\text{SOTR}}{P} \quad (4)$$

where P = power applied (kW).

2.1. Dimensional analysis

The aeration process depends on many factors such as volume of water, diameter of paddle wheel, size of paddle blade, presence of the baffles in the aeration tank, etc. Therefore, to study the performance of the aerator systems the above variables are to be considered in their dimensionless form, which are usually obtained from the dimensional analysis.

The oxygen transfer rate depends on the physical properties of water and air, the flow parameters, and the geometric parameters of the aerator system. For the purpose of clarity it may be divided into three classes:

Geometric variables: h = submergence depth of the paddle blades (L), b = breadth of the blade of the rotor (L), α = bent angle ($M^0 T^0 L^0$), l' = horizontal projection of bent length (L), s = impeller pitch (L), V = volume of water under aeration (L^3), l = length of the blade of the rotor (L), d = diameter of rotor (L).

Material variables: ρ_a = density of air ($M L^{-3}$), ρ_w = density of water ($M L^{-3}$), D_L = molecular diffusivity of oxygen in air ($L^2 T^{-1}$), v = kinematic viscosity of water ($L^2 T^{-1}$), σ = surface tension of water in contact with air ($M T^{-2}$).

Process variables: N = rotational speed (T^{-1}) and g = acceleration due to gravity ($L T^{-2}$).

Surface aeration process consists of creating air bubbles at the surface by churning action of the rotor blades. The value of the oxygen transfer rate should therefore, depend on the number of air bubbles per unit volume, size and distribution of these bubbles. But it is usually believed that these bubble parameters also depend on the same parameters as the rest of the parameters on which the oxygen transfer rate depends, viz. the physical properties of air and water, the flow parameters and the geometric parameters of the aeration system (Maise, 1970). Thus, the variables that can influence the oxygen transfer rate at 20 °C (i.e. SOTR)

may be expressed as a functional relationship for a given shape of aeration tanks as follows:

$$\mathrm{SOTR}/\Delta c = f_1(h, b, \alpha, l', s, V, l, d, N, g, \rho_a, \rho_w, \sigma, v, D_\mathrm{L}) \tag{5}$$

Based on the Buckingham π theorem, Eq. (5) may be expressed as,

$$Y = f_2(h/d, b/d, \alpha, l'/d, s/d, V/d^3, l/d, \rho_\mathrm{a}/\rho_\mathrm{w}, v/D_\mathrm{L}, N^2d/g, Nd^2/v, N^2d^3\rho/\sigma] \tag{6}$$

where

$$Y = \text{Absorption number} = \mathrm{SOTR} \times (v/g^2)^{1/3}/(\Delta c \times d^3) \tag{7}$$

$$N^2d/g = \text{Froude number, } Fr \tag{8}$$

$$Nd^2/v = \text{Reynolds number, } Re \tag{9}$$

$$N^2d^3\rho/\sigma = \text{Weber number, } We \tag{10}$$

$$v/D_\mathrm{L} = \text{Schmidt number, } Sc \tag{11}$$

The first seven dimensionless quantities govern the geometrical similarity of the system and the last three dimensionless quantities govern the dynamic similarity of the system. $\rho_\mathrm{a}/\rho_\mathrm{w}$ and Sc are invariant in the aeration tank and can be omitted from Eq. (6). No information is available regarding l/d, but for simplification of the problem its value was selected as 0.25 and kept constant throughout the study.

Many investigators believed that the influence of We is negligible in comparison with the influence of Re and Fr, so in the present investigation We is considered to be a parameter of secondary importance and dropped from Eq. (6).

Finally Eq. (6) can be expressed as,

$$Y = f_3(h/d, b/d, \alpha, l'/d, s/d, V/d^3, N^2d/g, Nd^2/v] \tag{12}$$

Similarly,

$$Ne = f_4(h/d, b/d, \alpha, l'/d, s/d, N^2d/g, Nd^2/v] \tag{13}$$

where

$$Ne = \text{Power number} = P/(\rho \times N^3 \times d^5) \tag{14}$$

SAE is the most important parameter for comparison of the performance of the aerators. Therefore, it is proposed to express SAE in a non-dimensional form by dividing the absorption number (Y) with power number (Ne) and can be termed as SAE′. Thus,

$$\mathrm{SAE}' = Y/Ne = (\mathrm{SOTR}/P) \times (v/g^2)^{1/3} \times (\Delta c \times d^3)^{-1} \times \rho \times N^3 \times d^5$$

or

$$\begin{aligned}\mathrm{SAE}' &= \mathrm{SAE} \times (v/g^2)^{1/3} \times (\Delta c)^{-1} \times \rho \times N^3 \times d^2 \\ &= f_5(h/d, b/d, \alpha, l'/d, s/d, V/d^3, N^2d/g, Nd^2/v]\end{aligned} \tag{15}$$

2.2. Geometric similarity

For an optimal solution of Eq. (15), one requires a specific set of values of the six non-dimensional geometric parameters: h/d, b/d, α, s/d, l'/d and V/d^3 such that a maximum oxygen transfer rate can be achieved for any given dynamic conditions as represented by the remaining two parameters (Fr and Re). Thus, an optimal solution to the geometrical similarity is essential, and such an exercise of finding optimal geometric similarity for maximum aeration was performed. The effect of each one of the governing dimensionless parameters on the dependent dimensionless parameter being studied was determined in the laboratory using a geometrically similar system. By varying only one governing dimensionless parameter at a time and observing the nature of variation of the dependent parameter with it, a single functional relationship between the dependent parameter and all the governing parameters could be established. This approach, however, has the limitation that the functional relationship so obtained is valid only for the ranges of the governing parameters studied. The schedule of experiments to obtain the specific optimum values for each of the geometric parameters, termed as Series G, is shown in Table 1. Series G1–G6 deal with the determination of optimum values of h/d, b/d, α, l'/d, s/d and V/d^3, respectively, for a particular dynamic condition.

2.3. Dynamic similarity

Once the specific values of the six non-dimensional geometric parameters are fixed, the value of Ne and SAE′ given by Eqs. (13) and (15), respectively, depend only on the dynamic parameters Fr and Re and thus Eq. (15) can be further written for the geometrically similar systems as:

$$Ne = f_6(Fr, Re) \tag{16}$$

$$\mathrm{SAE}' = f_7(Fr, Re) \tag{17}$$

The intensity of turbulence and wave action on the water are the major sources normally associated with surface aeration. Turbulence and viscous effects are generally described by the Reynolds number (Re), where the surface wave action is described by the Froude number (Fr). Hence both Re and Fr are important as far as the surface aeration is concerned. Eqs. (16) and (17) signify the dynamic similarities that require explicit solutions. While doing so, the concept of 'theoretical power per unit volume' was found to be very useful.

2.4. Power per unit volume concept

Many investigators have suggested (Connolly and Winter 1969; Horvath, 1984; Simha, 1991; Rao, 1999) that power per unit volume is a useful concept to simulate oxygen transfer in geometrically similar systems and this concept is utilised in the present studies. Power is required to agitate the water body in the tank by rotating the aerator blades. According to the basic hydrodynamic principles, the power P is

Table 1
Schedule of experiments—geometric similarity (Series G)

Series no.	Similarity conditions for the experiment	Variables	Range of the variable	Description of the setup	Objective of the experiment
G1	$l/d = 0.25$, $b/d = 0.25$, $\alpha = 45°$, $l'/d = 0.05$, $s/d = \pi/6$, $V/d^3 = 82.81$, $Fr \approx 0.1132$ and $Re \approx 310077.5$	h/d	0.025–0.225	For all the runs: $l = 100$ mm, $d = 400$ mm, $b = 100$ mm, $\alpha = 45°$, $l' = 20$ mm, $s = 66.67\pi$ mm, $V = 5.30$ m^3, $N = 100$ rpm	To fix up optimum value for h/d, i.e. (h/d)*
G2	$l/d = 0.25$, $h/d = (h/d)$*, $\alpha = 45°$, $l'/d = 0.05$, $s/d = \pi/6$, $V/d^3 = 82.81$, $Fr \approx 0.1132$ and $Re \approx 310077.5$	b/d	0.1–0.4	For all the runs: $l = 100$ mm, $d = 400$ mm, $h = (h)$*, $\alpha = 45°$, $l' = 20$ mm, $s = 66.67\pi$ mm, $V = 5.30$ m^3, $N = 100$ rpm	To fix up optimum value for b/d, i.e. (b/d)*
G3	$l/d = 0.25$, $h/d = (h/d)$*, $b/d = (b/d)$*, $l'/d = 0.05$, $s/d = \pi/6$, $V/d^3 = 82.81$, $Fr \approx 0.1132$ and $Re \approx 310077.5$	α	0–75°	For all the runs: $l = 100$ mm, $d = 400$ mm, $h = (h)$*, $b = (b)$*, $l' = 20$ mm, $s = 66.67\pi$ mm, $V = 5.30$ m^3, $N = 100$ rpm	To fix up optimum value for α, i.e. (α)*
G4	$l/d = 0.25$, $h/d = (h/d)$*, $b/d = (b/d)$*, $\alpha = (\alpha)$*, $s/d = \pi/6$, $V/d^3 = 82.81$, $Fr \approx 0.1132$ and $Re \approx 310077.5$	l'/d	0.025–0.075	For all the runs: $l = 100$ mm, $d = 400$ mm, $h = (h)$*, $b = (b)$*, $\alpha = (\alpha)$*, $s = 66.67\pi$ mm, $V = 5.30$ m^3, $N = 100$ rpm	To fix up optimum value for l'/d, i.e. (l'/d)*
G5	$l/d = 0.25$, $h/d = (h/d)$*, $b/d = (b/d)$*, $\alpha = (\alpha)$*, $l'/d = (l'/d)$*, $V/d^3 = 82.81$, $Fr \approx 0.1132$ and $Re \approx 310077.5$	s/d	$\pi/12$ to $\pi/4$	For all the runs: $l = 100$ mm, $d = 400$ mm, $h = (h)$*, $b = (b)$*, $\alpha = (\alpha)$*, $l' = (l')$*, $V = 5.30$ m^3, $N = 100$ rpm	To fix up optimum value for s/d, i.e. (s/d)*
G6	$l/d = 0.25$, $h/d = (h/d)$*, $b/d = (b/d)$*, $\alpha = (\alpha)$*, $l'/d = (l'/d)$*, $s/d = (s/d)$*, $Fr \approx 0.1132$ and $Re \approx 310077.5$	V/d^3	76.56–89.06	For all the runs: $l = 100$ mm, $d = 400$ mm, $h = (h)$*, $b = (b)$*, $\alpha = (\alpha)$*, $l' = (l')$*, $s = (s)$*, $N = 100$ rpm	To find the effect of V/d^3 on aeration process

* denotes the optimum values of the variables.

generally expressed as $P \propto Qh_f$, where Q is the discharge of water being pumped by the rotation of the impeller blades of dimensions b and l, and h_f is the head loss due to rotational movement of water in the tank. The characteristic tangential velocity of water v may be considered as proportional to Nd. Because of geometric similarity, $b \propto d$ and $l \propto d$, then the cross-sectional area of the blades $bl \propto d^2$. Therefore the water discharge due to the rotor action can be expressed as $Q \propto Nd^3$. The head loss h_f may be considered to be proportional to the velocity head $v^2/2g$, where $v \propto Nd$ and g is the gravitational constant. Therefore the power $P \propto N^3d^5$. For geometrical similar systems the volume of water in the tank $V \propto d^3$. Therefore, the power per unit volume, $P/V \propto N^3d^2$. As given in Eqs. (16) and (17), SAE′ and Ne depend on both Fr and Re under geometrically similar conditions, the dimensional parameter N^3d^2 is converted to a non-dimensional parameter, X, by expressing it in terms of $Fr = N^2d/g$, and $Re = Nd^2/v$ as:

$$X = N^3d^2(g^{4/3}v^{1/3}) = Fr^{4/3}Re^{1/3} \tag{18}$$

This parameter X is considered as the parameter representing the theoretical power per unit volume and it includes the effect of Fr and Re simultaneously. For total dynamic similitude among the geometrically similar systems, it is impossible to maintain both Fr and Re as invariant because air and water are used in all the experiments. If the Reynolds criterion is followed to simulate SAE′ for a given size of aerator, then the value of SAE′ thus obtained cannot be the same in other sizes. Because of non-compliance of the other parameter Fr, SAE′ can thus be affected by the size of the aerator. A similar effect can be explained while following the Froude criterion. This is called the scale effect. To avoid such scale effects, X, the parameter governing the theoretical power per unit volume (Eq. (18)), which includes the effect of both Fr and Re was considered to simulate the oxygen transfer in geometrically similar systems. The ranges of data of different variables along with the experimental conditions for uniquely simulating the oxygen transfer in geometrically similar systems termed as Series D are presented in Table 2.

2.5. Experimental set-up

To investigate the effects of the geometric and the dynamic variables on surface aeration process, two unbaffled tanks of dimensions $2.9 \times 2.9 \times 1.6$ and $5.9 \times 2.9 \times 1.6$ m were used. A line sketch of the aeration unit showing the sectional view is presented in Fig. 1. Paddle blades were made of mild steel sheet of thickness 2 mm. The different dimensions of the paddle blades are shown in Table 1. Collar was made of mild steel with inner and outer diameter of 25.4 and 35.4 mm, respectively. An arrangement was made to attach the number of spokes as per requirement by means of nuts and bolts. The blades could also be attached to the spokes by means of nuts and bolts. The spokes were so arranged as to have equal angular interval from each other. For providing the necessary variable speed, DC shunt wound type flange mounted motor (Make: General Engineering and Electrical Works, Calcutta) of 2 hp capacity was used. The speed variation (0–1500 rpm) was obtained by varying the armature voltage through a multi-turn potentiometer with the help of

Table 2
Schedule of experiments—simulation of oxygen transfer (Series D)

Sl. No.	Range of the variables				Number of experiments	Dimensions of experimental tank	Geometric similarity conditions for the experiments
	d (mm)	N (rpm)	Re	Fr			
D1	400	70–120	217054.3–372093	0.055499–0.163099	11	$2900 \times 2900 \times 1600$ mm	$I/d = 0.25$, $h/d = (h/d)^*$, $b/d = (b/d)^*$, $\alpha = (\alpha)^*$, $l'/d = (l'd)^*$, $s/d = (s/d)^*$ $V/d^3 = (V/d^3)^*$
D2	425	70–120	245033.9–420058.1	0.058968–0.173293	11		
D3	450	70–120	274709.3–470930.2	0.062436–0.183486	11		
D4	475	70–120	306080.4–524709.3	0.065905–0.19368	11		
D5	500	70–120	339147.3–581395.3	0.069374–0.203874	11	$5900 \times 2900 \times 1600$ mm	
D6	550	70–120	410368.2–703488.4	0.076311–0.224261	11		
D7	600	70–120	488372.1–837209.3	0.083248–0.244648	11		

thyristor converter. The thyristor converter runs on an input voltage of 440 V, 3 A and gives DC output of 220 V, 5.5 A to the motor. Adaptable speed reduction unit of worm and worm wheel type (Make: M/s Greaves Ltd, Pune), fully oil cooled of standard gear ratio 7.5:1 was used to obtain the desired speed from DC Motor output shaft. The input shaft of the gearbox was directly coupled with the motor and the output horizontal shaft was coupled with the aerator shaft for experiment. The aerator shaft was supported by ball bearing. Other end of the aerator shaft carries the paddle blades. Diameter of the shaft is 25.4 mm and the length is 1.05 m. To keep the aerator shaft in proper alignment, one ball bearing was placed in the slot provided in the raised frame. Two couplings were used to join the motor shaft and gearbox input shaft and the gearbox output shaft and aerator shaft.

An arrangement was made so that by sliding the whole unit the depth of submergence could be varied. For this purpose base and top frame of dimensions $365 \times 315 \times 50$ mm made of angle iron of size $50 \times 50 \times 5$ mm were used. The base frame was fixed by means of grouted bolts of 9.5 mm diameter and 100 mm length. Four bushes, each of inner and outer diameters as 50 and 60 mm, respectively, and 53 mm long were welded to the base frame. Four GI pipes having inner and outer diameters and length of 40, 47 and 2030 mm, respectively, were used for free vertical movement of the aerator unit. The pipes were welded to the base and top frame bushes to avoid vibration of the aeration system during running. Further to reduce the shock effect, the top frame was bolted with two mild steel angles which were supported on the side walls. One U-Channel of size $200 \times 80 \times 6$ mm was

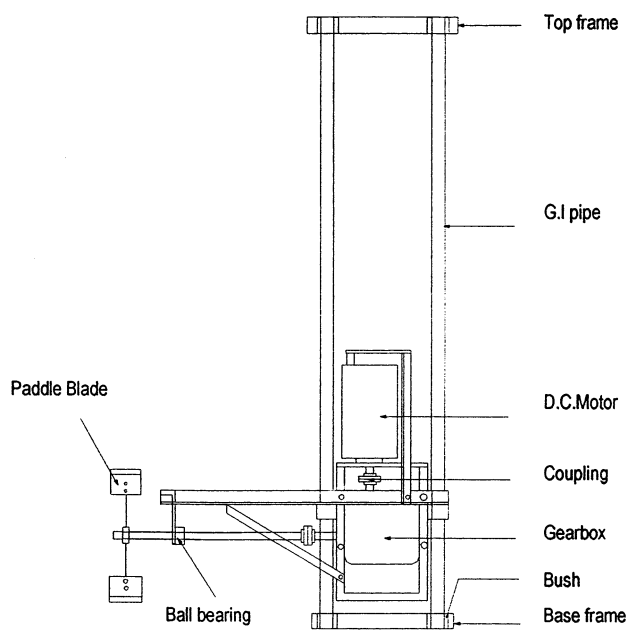

Fig. 1. Line diagram of aeration unit.

placed on two brick masonry pillars and a U hook to hold a chain-pulley system was provided in it such that its position coincided with the centre of the top frame. To avoid bending of the aerator shaft, one bearing block was provided at a distance of 900 mm from the coupling. The bearing block was supported by an angle bracket welded to two angles of size $50 \times 50 \times 5$ mm. These angles were bolted with the gearbox frame. One chain pulley block of triple spur gear type was used for lifting the motor and gearbox unit to get the desired submergence depth.

2.6. Measurement of available power at the shaft

One AC/DC ammeter of model MIA class (1.0) ISI 248-68 and an AC/DC voltmeter of model MIA class (1.0) ISI 248-68 were used to measure the current and voltage, respectively. The revolution of the motor shaft was measured by using digital frequency counter. The power available at the shaft was calculated by measuring input power and deducting the losses occurring in the DC Motor. Since the range of speed of rotation of shaft is low (70–120 rpm) only the important losses, viz. copper and iron losses were considered for determining the power available at the shaft. To determine these losses, current and voltage at no load (free rotation of paddle wheel without load) condition and loaded condition (with water) were measured during the experiment. Then the power available at the shaft was calculated as follows (Cook and Carr, 1947). From the measurement of no load current (I_1) and voltage (V_1) the iron loss was calculated by

$$I_L = l_1 \times V_1 - l_1^2 \times R_a \tag{19}$$

where R_a = armature resistance of the DC Motor and $I_1^2 \times R_a$ is no load copper loss. From the measured loaded condition current, I_2, and voltage, V_2 the copper loss was calculated by

$$C_L = l_2^2 \times R_a \tag{20}$$

$$\text{Total loss occurring in DC Motor, } T_L = I_L + C_L \tag{21}$$

$$\text{Incoming power to DC Motor } P_1 = l_2 \times V_2 \tag{22}$$

$$\text{The power available at the shaft, } P_S = P_1 - T_L \tag{23}$$

2.7. Aeration test

Standard oxygen transfer tests were conducted in tanks of clean tap water under standard conditions (20 °C and 760 mmHg). At first the water in the tank was deoxygenated by applying cobalt as cobalt chloride ($CoCl_2$) and sodium sulphite (Na_2SO_3). The aerator being tested was used to mix cobalt chloride and sodium sulphite with the water. The aerator was run until the DO was reduced to below 0.2 mg/l. When the DO concentration again began to rise, readings were taken at timed intervals till DO increased from 0% saturation to at least 80% saturation. At least 15 DO measurements at equal time intervals were taken. Century make DO meter (model CMK 731) was used to measure the DO concentration in water. The overall oxygen transfer coefficient was then calculated from the equation:

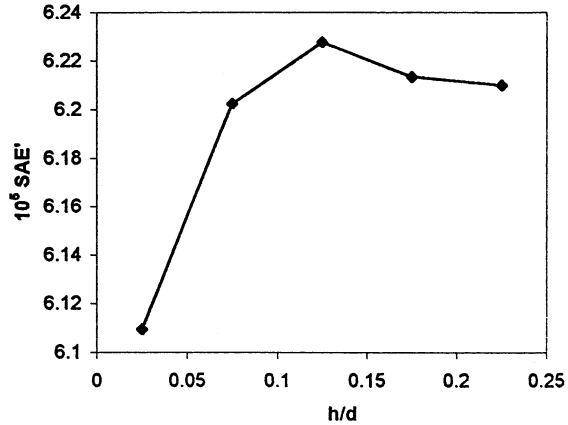

Fig. 2. Variation of SAE′ with h/d.

$$k_L a = \frac{\ln \mathrm{OD}_1 - \ln \mathrm{OD}_2}{(t_2 - t_1)/60} \tag{24}$$

where $k_L a$ = overall oxygen transfer coefficient (h^{-1}), OD_1 = oxygen deficit ($C_s - C_1$) at time t_1 (mg/l), OD_2 = oxygen deficit ($C_s - C_2$) at time t_2 (mg/l), C_s = DO concentration at saturation for tank water (mg/l), C_1 = measured DO concentration at time t_1 (mg/l), C_2 = measured DO concentration at time t_2 (mg/l), t_1 = time 1 (min) and t_2 = time 2 (min). $k_L a$ was calculated by plotting a graph of time versus the natural log of the oxygen deficit. The plot produced a straight line with a negative slope. By selecting two points on the line, usually at about 10 and 70% of saturation, the slope of the line could be obtained. The slope of the line is the overall oxygen transfer coefficient, $k_L a$. The SOTR and SAE were calculated from Eqs. (3) and (4), respectively.

3. Results and discussion

The results obtained from the study are presented and discussed in this section.

3.1. Optimal geometric parameters

The experimental details for obtaining optimal geometric parameters (Series G) are presented in Table 1. The variation of SAE′ with h/d, b/d, α, l'/d, s/d and V/d^3 are shown in Figs. 2–7, respectively. In these sets of experiments SAE′ is proportional to SAE as paddle wheel speed (N) and the diameter (d) of the aerator were kept constant and the other variables on which SAE′ depends are also constant for a particular temperature. Hence the values of the geometric dimensionless parameters represent the optimum geometric parameters of the paddle wheel aerator at a particular dynamic condition for which the SAE is maximum. It can be noticed from the figures that the optimum geometric parameters of the paddle wheel at a particular dynamic condition ($Re \approx 310077.5$ and $Fr \approx 0.1132$) are as follows:

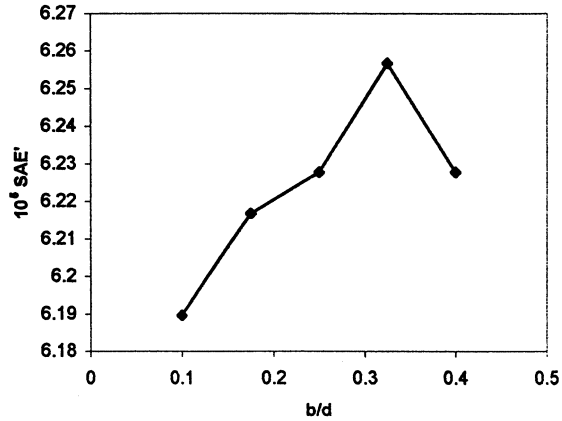

Fig. 3. Variation of SAE′ with b/d.

$h/d = 0.125$, $b/d = 0.325$, $\alpha = 45°$, $l'/d = 0.0625$, $s/d = 0.5238$, i.e. $\pi/6$ and $V/d^3 = 82.81$ (25)

3.2. Dynamic similarity

For total dynamic similitude, among the geometrically similar systems, it is impossible to maintain both *Re* and *Fr* as invariant because air and water were used in all the aeration tests. If the Reynolds criterion is followed to simulate SAE′ or *Ne* for a given size of aerator, then such a result of SAE′ or *Ne* cannot be the same for other sizes (for the same *Re*). Because of non-compliance of the other parameter *Fr*,

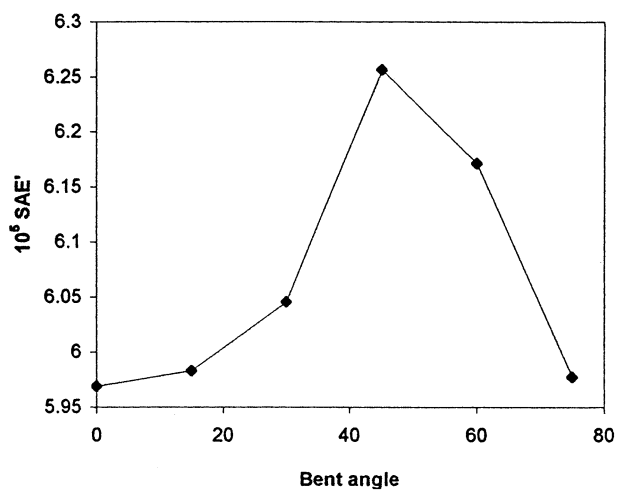

Fig. 4. Variation of SAE′ with bent angle.

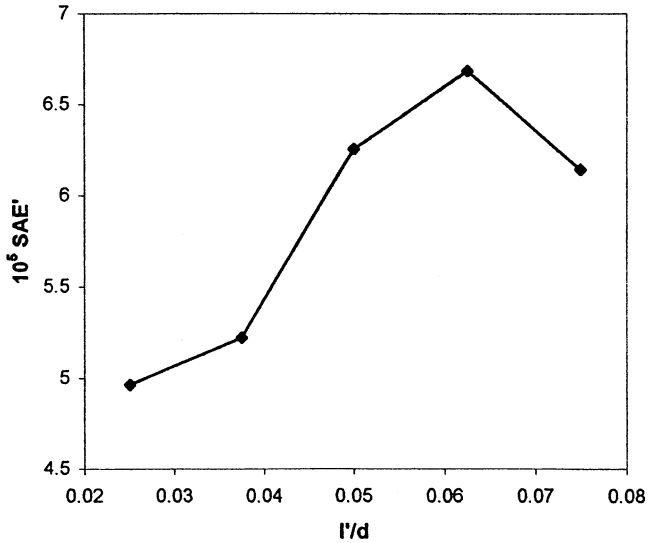

Fig. 5. Variation of SAE′ with l'/d.

SAE′ or *Ne* can thus be affected by the size or scale of the aerator. A similar effect can be explained while following the Froude criterion. This is called the 'scale effect'.

3.3. Scale effects

Fig. 8 shows a plot between SAE′ and *Re* for seven different sizes of paddle wheels. The data from each paddle wheel size fall separately on different parallel

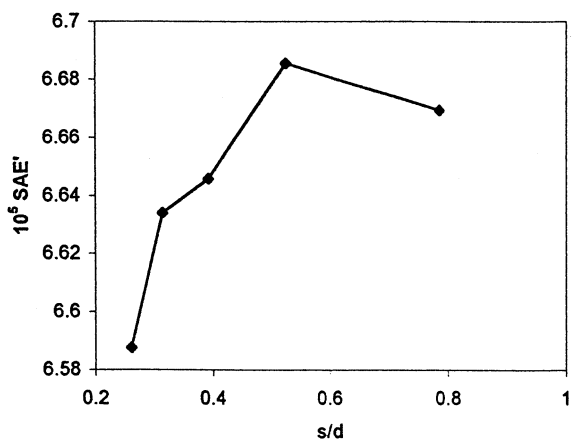

Fig. 6. Variation of SAE′ with s/d.

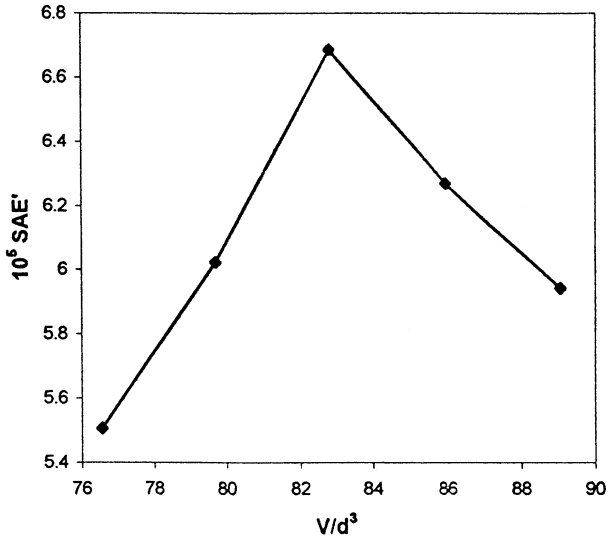

Fig. 7. Variation of SAE' with V/d^3.

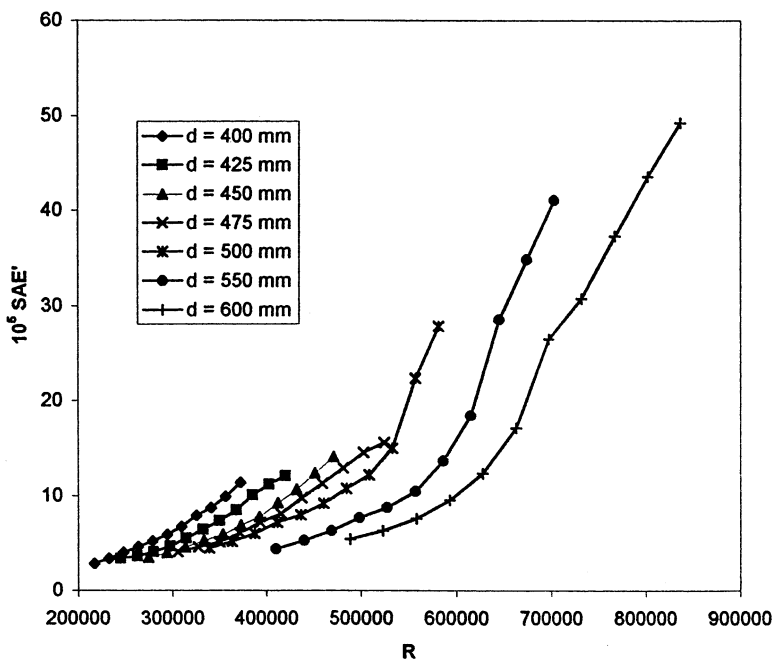

Fig. 8. Scale effects on SAE′ due to Reynolds criterion.

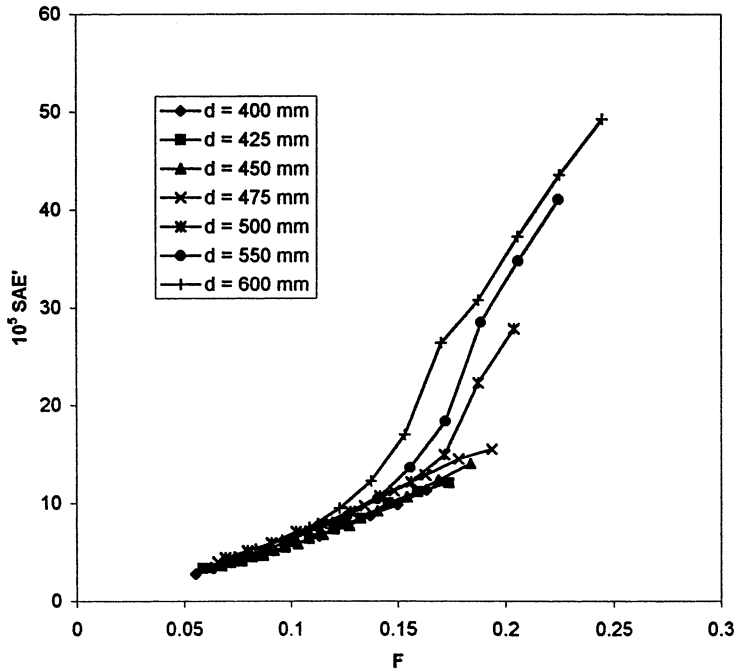

Fig. 9. Scale effects on SAE′ due to Froude criterion.

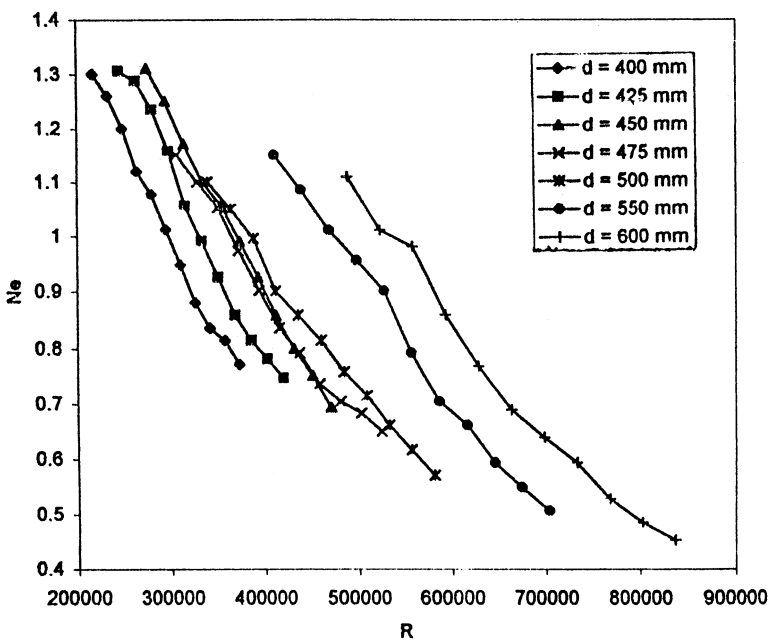

Fig. 10. Scale effects on Power number (*Ne*) due to Reynolds criterion.

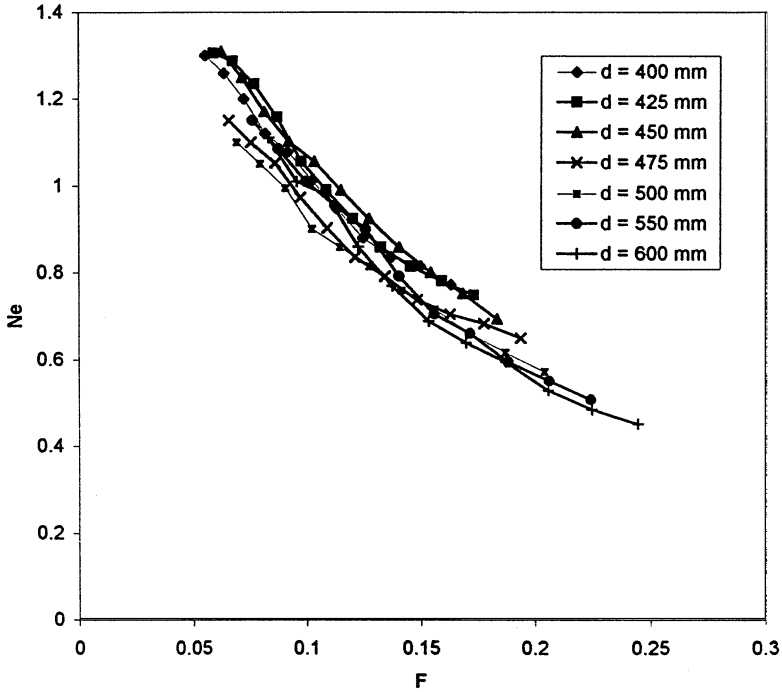

Fig. 11. Scale effects on Power number (*Ne*) due to Froude criterion.

curves indicating the size or scale effect on SAE′. It can be observed from Fig. 8 that for any given *Re*, the value of SAE′ increases significantly as the paddle wheel size decreases, and as such the scale effects are predominantly visible.

A similar exercise was done to demonstrate the Froude criterion and associated scale effects on SAE′ as shown in Fig. 9. For a given *Fr*, the values of SAE′ increase with the increase of the paddle wheel size. This observation is inverse to the Reynolds criterion (Fig. 8). Curves for different sizes of paddle wheels in Fig. 9 are closer to each other when compared with the closeness of curves in Fig. 8 which indicates that the scale effects are more pronounced in the Reynolds criterion, whereas they are less pronounced in the Froude criterion between paddle wheels of various sizes.

Similarly from Figs. 10 and 11 it can be noticed that the values of *Ne* for different sizes of paddle wheel fall on separate curve due to the Reynolds and Froude criterion, respectively. It can also be noticed that the scale effects are much less pronounced in Froude criterion than the Reynolds criterion.

3.4. Simulation equation for oxygen transfer and power consumption

A plot was made between SAE′ and *X*, the non-dimensional parameter governing the theoretical power per unit volume as shown in Fig. 12 to simulate the oxygen transfer mechanism. It is quite interesting to note that the entire set of data points

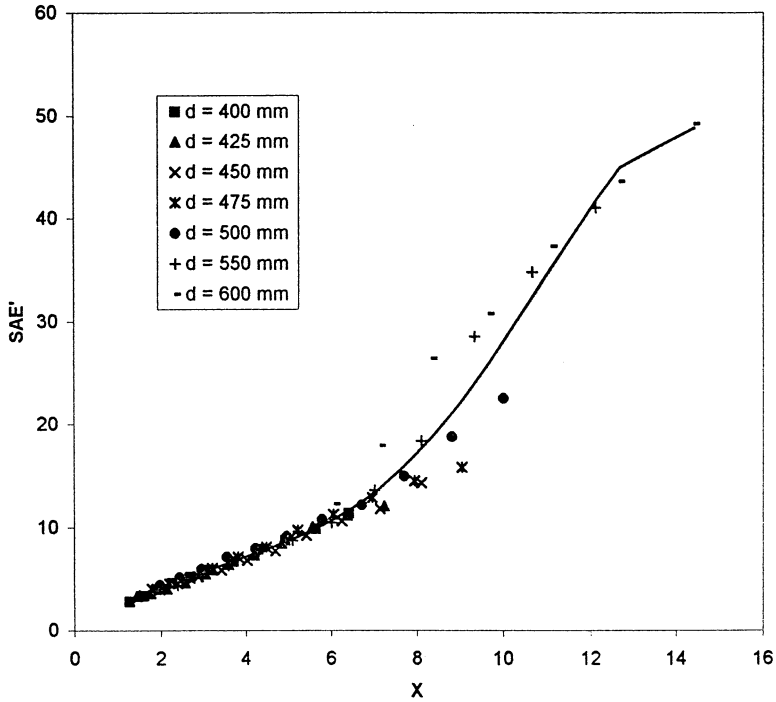

Fig. 12. Simulation of oxygen transfer under geometric similar conditions.

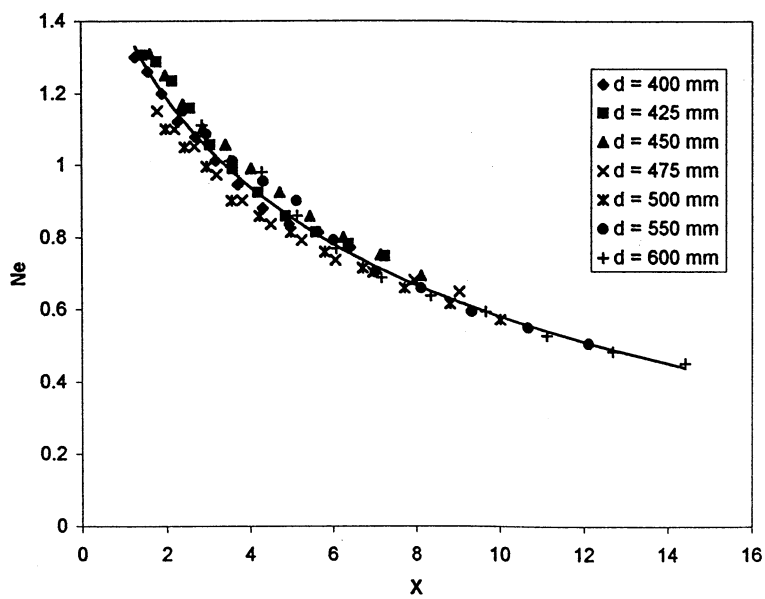

Fig. 13. Simulation of power consumption under geometric similar conditions.

for all sizes of paddle wheels fall very closely on a single curve suggesting unique relationship between SAE′ and X, as long as the non-dimensional scales according to Eq. (25) are maintained. In Fig. 12, the following equation fits quite well for the entire range of data points:

$$\mathrm{SAE}' = \{-147.48 \times e^{(0.151X)} + 0.176(X)^{3.13} + 178.48 + 33.84X - 9.03 \times \ln(67.51X)\} \times 10^{-5} \quad (r^2 = 0.966) \tag{26}$$

Eq. (26) includes the effects of both Reynolds and Froude numbers and hence it is proposed as the simulation equation for oxygen transfer in geometrically similar systems, which confirms quantitatively that SAE′ can be simulated with power per unit volume.

Another plot was made between Ne and X (Fig. 13) to obtain the power correlation for different sizes of paddle wheels. In this case also it is found that all the data points for different paddle wheel sizes fall very closely on a single curve. The following equation fits well for the entire range of data points.

$$Ne = 0.434 \times e^{(-0.232X)} + 16.95(X)^{-0.0107} - 15.89 - 0.0111X \quad (r^2 = 0.969) \tag{27}$$

Eqs. (26) and (27) represents the simulation equations for oxygen transfer and power consumption, respectively.

3.5. Analysis

It is worth discussing the simulation of oxygen transfer and power consumption in geometrically similar systems as represented by Eqs. (26) and (27) on various aspects such as the following: (1) goodness-of-fit when compared to various sources of unavoidable errors in the measurement of experimental variables; (2) characteristic features of the simulation curve; and (3) scale effects on SAE′ and Ne, when the Reynolds and the Froude criteria are followed.

3.6. Experimental errors versus Eqs. (26) and (27)

It is appropriate to discuss the various measurements and accuracies of the experimental data for which Eqs. (26) and (27) are fitted. All of the linear dimensions of the geometric elements of the aeration tank are fixed with an accuracy ranging from ± 0.1 to ± 2 mm. The dimensions b, l and l' have an accuracy of ± 0.1 mm, whereas d, s and h have an accuracy ± 1 mm. The bent angle α of the paddle blades has an accuracy of $\pm 0.5°$. The tanks of sizes $5900 \times 2900 \times 1600$ and $2900 \times 2900 \times 1600$ mm are made of brick masonry with a smooth cement plastering on the inside surface and thus the accuracy of their linear dimensions is ± 2 mm. These errors in measurements are to be reflected slightly in the values of the seven non-dimensional geometric variables in Eq. (6). The paddle wheel speed N in rpm is subjected to an error of about $\pm 0.5\%$ during the period of experimentation and this error is mainly due to inherent problem associated with the electrical and mechanical system of the motor and aerator. The accuracy of

measurement of DO concentration in water samples is ± 0.1 ppm and the time intervals t of taking water samples are subjected to an error of about ± 3 s. The water temperature T is measured with an accuracy of ± 0.1 °C and the kinematic viscosity v is taken from standard tables based on the water temperature. Moreover, the physical roughness on the inside surface of the tank surface is another important variable that can influence the oxygen transfer coefficient because the turbulent intensities can be influenced by the physical roughness (Rao, 1999). In the present experiments, the inside surfaces of the tanks are fairly smooth and it is presumed that roughness effects are uniform for all of the dynamic conditions in both the tanks.

All such errors are gradually integrated into Eq. (1) while determining $k_L a_T$ and fortunately, while doing the regression analysis of Eq. (1), all of these errors are apparently smoothed out and a reasonably good estimate of $k_L a_{20}$ is thus made possible. Also all such errors are likely to affect *Re* and *Fr* as well. It is difficult to avoid such errors, and at the same time it is equally difficult to estimate the effect of such errors. However, the data scatter in Figs. 12 and 13 are very small and negligible and hence one may come to a conclusion that the aforementioned various errors are tolerable.

The form of the simulation equations as given in Eqs. (26) and (27) are derived based on intuition and followed up with suitable regression analysis. The equations thus fitted work reasonably well and it is estimated that Eqs. (26) and (27) predict the values of $k_L a_{20}$ and P with an average error of ± 0.88 and $\pm 0.16\%$, respectively, when compared with the experimentally determined values. Thus Eqs. (26) and (27) are justifiable by taking into consideration all of the experimental errors themselves. Therefore, Eqs. (26) and (27) may be used with confidence for predicting the aeration performance.

4. Conclusions

A non-dimensional technique was applied to predict the aeration performance of paddle wheel aerators and reasonably good results were obtained. Non-dimensional numbers relating to standard aeration efficiency (SAE), effective power (P) and theoretical power per unit volume (P/V) termed as SAE′, *Ne* and X, respectively, were proposed. An optimal geometric similarity of various linear dimensions of the paddle wheel was established (Eq. (25)). Also it has been established that neither the Reynolds criterion nor the Froude criterion is singularly valid to simulate either SAE′ or *Ne*, simultaneously for different sizes of aerators, even though they are geometrically similar. Occurrence of scale effects due to the Reynolds and the Froude laws of similitude on both SAE′ and *Ne* were evaluated. Simulation equations (Eqs. (26) and (27)) uniquely correlating SAE′, *Ne* and X were developed which can predict the values of SAE, effective power (P) and standard oxygen transfer rate (SOTR) for different values of paddle wheel diameter (d) and paddle wheel speed (N).

Acknowledgements

Thanks are due to the Agricultural and Food Engineering Department, IIT, Kharagpur where aeration tests were performed. The authors are also grateful to the Indian Council of Agricultural Research (ICAR), F. No. 4-97/95-AE, dated 23.05.96 for providing the financial support.

References

Ahmad, T., Boyd, C.E., 1988. Design and performance of paddle wheel aerators. Aquacult. Eng. 7 (1), 39–62.

Banks, R.B., Sally, L.R., Polprasert, C., 1983. Mechanical mixing and surface reaeration. J. Environ. Eng., ASCE 109 (1), 232–241.

Boyd, C.E., Ahmad, T., 1987. Evaluation of Aerators for Channel Catfish Farming. Bulletin 584. Alabama Agricultural Experiment Station. Auburn University, AL.

Boyd, C.E., 1998. Pond water aeration systems. Aquacult. Eng. 18, 9–40.

Cleasby, J.L., Baumann, E.R., 1968. Oxygenation efficiency of a bladed rotor. J. Water Pollut. Contr. Fed. 40, 412–424.

Connolly, J.R., Winter, R.L., 1969. Approaches to mixing operation and scale-up. Chem. Eng. Prog. 65 (8), 70–78.

Cook, A.L., Carr, C.C., 1947. Elements of Electrical Engineering, 5th ed. Wiley, New York.Eckenfelder Jr., 1956. Process design of aeration system for biological waste treatment. Chem. Eng. Prog. 52 (7), 286–292.

Eckenfelder Jr., O'Conner, 1961. Biological Waste Treatment. Pergamon, Tarrytown, NY.

Horvath, I., 1984. Modelling in the Technology of Wastewater Treatment. Pergamon, Tarrytown, NY.

Knight, R.S., 1965. MS Thesis. Iowa State University, Ames, IA.

Kolega, J.J., Nelson, G.L., Graves, Q.B., 1969. Analysis for oxygen transfer coefficients in rotor aeration systems. Animal Waste Management: A conference on Agricultural Waste Management, 1968. Cornell University, Ithaca, NY.

Lewis, W.W., Whiteman, W.G., 1924. Principles of gas absorption. Ind. Eng. Chem. 16 (2), 1215–1220.

Maise, G., 1970. Scaling methods for surface aerators. J. Sanitary Eng. Div. ASCE 96 (5), 1079–1083.

Manual of practice for water pollution control, 1988. Aeration a waste water treatment process. Water Environment Federation, Alexandria, VA, and ASCE, NY.

Matcalf & Eddy Inc., 1979. Waste Water Engineering: Treatment Disposal and Reuse. Tata McGraw-Hill, New Delhi.

Moore, J.M., Boyd, C.E., 1992. Design of small paddle wheel aerators. Aquacult. Eng. 11, 55–69.

Ognean, T., 1993. Aspects concerning scale-up criteria for surface aerators. Water Res. 27 (3), 477–484.

Rao, A.R., 1999. Prediction of reaeration rates in square, stirred tanks. J. Environ. Eng. 125 (3), 215–223.

Rappaport, U., Sarig, S., Marek, M., 1976. Results of tests of various aeration systems on the oxygen regime in the genosar experimental ponds and growth of fish there in 1975. Bamidgeh 28, 35–49.

Schmidtke, N.W., Horvath, T., 1976. Scale-up methodology for surface aerated reactors. Prog. Water Technol. 9, 477.

Simha, L.U., 1991. PhD Thesis. Department of Civil Engineering, Indian Institute of Science, Bangalore, India, 187pp.

Walker, P.G.W., 1962. Rotor aeration of oxidation ditches. Water Sewage Works 109, 238–241.

Wyban, J.A., Pruder, G.D., Leber, K.M., 1989. Paddlewheel effects on shrimp growth, production and crop value in commercial earthen ponds. J. World Aquacult. Soc. 20, 18–23.

Zlokarnik, M., 1979. Scale-up of surface aerators for wastewater treatment. Adv. Biochem. Eng. 11, 157–179.